Anisotropic photoluminescence properties of oriented poly(*p*-phenylene-vinylene) films: Effects of dispersion of optical constants

Cesare Soci,[1,2,*] Davide Comoretto,[3,4] Franco Marabelli,[2,4] and Daniel Moses[1]
[1]*Center for Polymers Organic Solids, University of California Santa Barbara, California 93106-5090, USA*
[2]*Dipartimento di Fisica "A. Volta," Università di Pavia, 27100 Pavia, Italy*
[3]*Dipartimento di Chimica e Chimica Industriale, Università di Genova, 16146 Genova, Italy*
[4]*National Laboratory for Ultrafast and Ultraintense Optical Science (ULTRAS), CNR-INFM, Italy*
(Received 4 October 2006; revised manuscript received 3 December 2006; published 13 February 2007)

We report on the effects of dispersive optical constants on the anisotropic photoluminescence spectra of highly oriented poly(*p*-phenylene-vinylene) films. Polarized transmittance, reflectance, and photoluminescence (PL) spectra have been measured over a broad spectral range, at different temperatures. Due to the high degree of chain orientation in the polymer films, the emission properties are highly anisotropic. The PL spectral shape and external quantum efficiency are significantly affected by self-absorption inside the polymer film and by refractive effects at the polymer-air interface. In order to elucidate these aspects we have determined the dispersion of the parallel and perpendicular components of the complex dielectric constant $(\varepsilon_1+i\varepsilon_2)$, by which the PL spectra have been corrected according to Fresnel equations. After correction, the PL intensity is found to be higher when the excitation is polarized perpendicular to the stretching direction, a fact that we attribute to charge-induced PL quenching. We have also considered the influence of the refractive index on the PL spontaneous emission rate and on the light extraction from the polymer film. The spectral dependence of the emission anisotropy functions of the corrected PL spectra indicates the presence of two distinct emitting species, which may originate from intramolecular and intermolecular states.

DOI: 10.1103/PhysRevB.75.075204 PACS number(s): 78.20.−e, 78.20.Ci, 78.40.Me, 78.55.Kz

I. INTRODUCTION

During the last three decades, conjugated polymers have attracted much attention thanks to their processing advantages for the realization of cost-effective electronic devices such as LEDs, FETs, and photovoltaics. Amongst their advantages, conjugated polymers offer the opportunity to obtain highly ordered structures that self-assemble on a molecular scale.[1] However, in polymer-based devices, the typical random coil conformation of the polymer chains hinders the intrinsic anisotropy of the electronic states. In spin-coated and drop-cast films, the preferential alignment of the polymer chains in the plane of the substrate often results in slight uniaxiality and optical anisotropy, with the ordinary refractive index in the plane of the substrate and the extraordinary refractive index perpendicular to the plane of the substrate.[2,3] Another way to achieve highly oriented materials, in which the macromolecules are chain extended and aligned, is through tensile drawing of the polymers or their nonconjugated precursor derivatives.[4] In such oriented samples the mechanical, electrical, and optical properties become more and more anisotropic as the degree of chain alignment and chain extension is improved.[5–8] Oriented films, where the photo- (electro-) luminescence is highly polarized, have been studied extensively for their potential application as retro illuminators in liquid-crystal displays.[9,10]

Poly(*p*-phenylene-vinylene) (PPV) and its substituted soluble derivatives are amongst the most widely utilized conjugated polymers as they show both good photoluminescence and charge-transport properties.[11,12] The availability of highly oriented PPV samples[13–15] has recently allowed us to clarify some fundamental issues such as the assignment of the polarized optical-absorption spectra, and the determination of the anisotropic dielectric functions.[2,3,16–18] Despite the massive work reported on oriented polymer films so far,[13–15,19–29] a general understanding of the processes underlying their electro-optical response has not yet been achieved. For instance, recent studies on the optical properties of unoriented PPV derivatives have questioned the character of the emitting excitons (i.e., intrachain vs interchain), indicating that intermolecular interactions, both in solution[30] and in silica nanoparticles composites,[31,32] may significantly affect the absorption[33,34] and the emission spectra.[35]

In order to clarify these issues, a detailed knowledge of the polymer optical constants is required.[16,36–38] Indeed, the dispersion of the complex refractive index affects the emission properties in several ways:

(1). It modifies the external PL spectral shape and quantum efficiency (QE) as the emitted light is self-absorbed and refracted on its way out of the polymer film.

(2). It influences the internal emission rate through the phase propagation of the emitted electromagnetic wave in the medium surrounding the emitters and through local-field effects.

(3). It affects light extraction from the polymer films.

In the following study we present a detailed analysis of the anisotropic optical constants of PPV films oriented by tensile drawing at high stretching ratio, and their effects on the emission properties at different temperatures. Transmittance, reflectance, and external PL emission spectra and quantum efficiency have been measured for different polarizations with respect to the stretching direction. In order to evaluate the effects of the optical constants dispersion on the emission properties, we have applied a data-reduction method recently developed in our group to determine the anisotropic dielectric constants of PPV with high accuracy

(0.1%); the resulting optical functions have been then utilized to derive the spectral dependence of the emission probability as a function of excitation and emission polarization, by means of a newly developed ray-optics model. After corrections, we find a higher-emission efficiency for excitation polarized perpendicular to the stretching direction, a fact that we attribute to charge-induced exciton quenching. Moreover, the PL anisotropy is spectrally dependent, while the high-energy emission is mainly polarized along the polymer-chain direction, indicating the intramolecular character of the emitting species, the anisotropy is reduced at low energy, thus suggesting a possible role of intermolecular interactions. The quantitative analysis of the emission anisotropy and the nature of photoexcitations in PPV are discussed.

II. EXPERIMENTAL METHODS

Thick (15.1 μm), free-standing PPV films were oriented by tensile drawing, with an elongation ratio of $l/l_0=5$, which is higher compared to the samples used in previous studies by our group.[16,39] The details of the polymer synthesis and film preparation are described elsewhere.[40–42]

Transmittance (T), reflectance (R), and diffuse reflectance spectra were recorded by a double-beam, double-monochromator spectrophotometer (Varian Cary 5E), equipped with a closed-cycle liquid-helium cryostat. The samples were kept in an inert atmosphere of helium gas during the measurements. A Glan-Taylor polarizer was mounted in the sample optical path, and the system response was taken into account recording a reference scan before each run; the parallel and perpendicular components of transmittance, reflectance, and of the derived optical constants are referred to the stretching direction of the polymer film, and denoted by $\parallel$ and $\perp$, respectively.

Diffuse reflectance spectra were collected by means of an integrating sphere and normalized to a standard polytetrafluoroethylene powder reference. In order to account for the light scattering caused by the film roughness (the formation of surface grooves upon tensile drawing at high-elongation ratios strongly enhances light scattering), specular, diffuse, and the sum of specular and diffuse reflectance were measured independently and utilized to normalize the specular reflectance obtained by the automatic spectrophotometer. The overall effect of light scattering is to reduce the intensity of the reflectance and transmittance of oriented PPV by about 10%.

Photoluminescence (PL) measurements were performed exciting the samples with the 458 nm line of an Ar^+ laser ($I=0.075$ mW, incidence angle 45°), while the samples were placed on a cold finger in the vacuum chamber of a cryostat, pumped to a pressure of $P<10^{-4}$ Torr. Part of the PL emission was collected (collection angle 45°), dispersed by a monochromator, and recorded by a CCD camera. A Fresnel prism was used to rotate the pump-laser polarization, and a polarizing sheet was used in front of the monochromator to determine the polarization of the emitted light; the emission spectra were corrected for the anisotropic response of the measuring system, calibrated with an additional light source positioned in the sample chamber. In presenting the PL data,

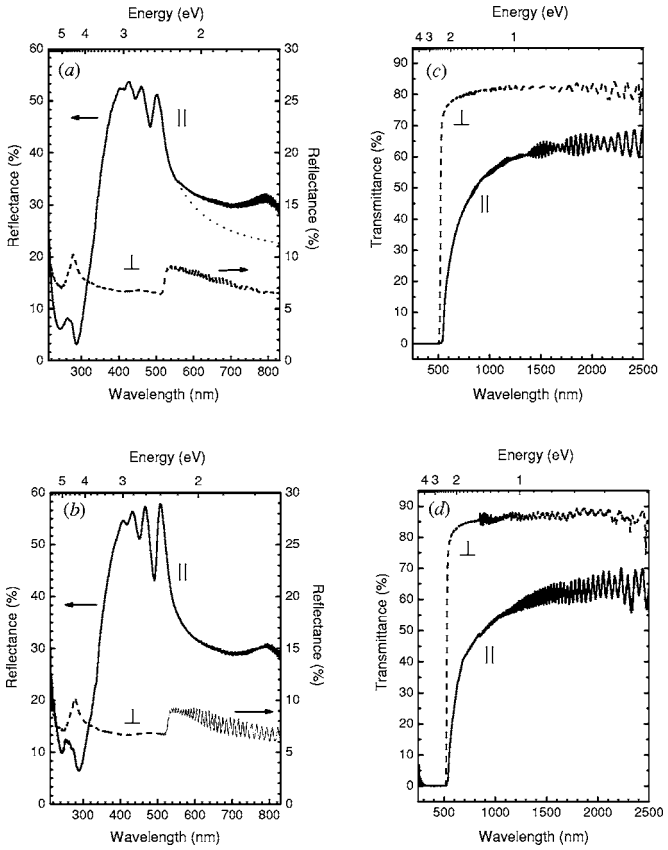

FIG. 1. Polarized reflectance [(a) and (b)] and transmittance [(c) and (d)] spectra of highly oriented PPV at room temperature [(a) and (c)] and 80 K [(b) and (d)]. Solid lines: polarization parallel to the draw axis; dashed lines: polarization perpendicular to the draw axis. The dotted line in panel *a* is the reflectance calculated from the optical constants in Fig. 3(a).

the four polarization combinations are denoted by (a,b), where the first symbol refers to the excitation polarization ($a=\perp$ or $\parallel$) and the second symbol indicates the emission polarization ($b=\perp$ or $\parallel$), relative to the stretching direction.

External photoluminescence quantum-efficiency measurements were performed following the procedure outlined by Greenham *et al.*[43] The excitation was provided by the UV line of the Ar^+ ion laser ($\lambda=363$ nm); the absolute absorbance of the sample was obtained independently by measuring the UV output of the integrating sphere after direct and indirect excitation of the sample.

III. RESULTS AND DISCUSSION

A. Absorbance and reflectance

Figure 1 shows the polarized reflectance spectra of oriented PPV obtained at room temperature [Fig. 1(a), solid line] and 80 K [Fig. 1(b)]. The reflectance spectra show similar characteristics to those previously observed in PPV:[16,39] At room temperature, the lowest-energy peak appearing at 500 nm in the parallel ($\parallel$) reflectivity is due to the π-π^* delocalized transition, which is strongly polarized along the polymer-chain axis.[44–56] The location of this purely

electronic transition (0-0) is comparable to that observed in high-quality, unoriented PPV samples obtained by improved synthesis,[57] thus indicating a remarkably long conjugation length facilitated by chain ordering. The 0-0 transition is followed by a well-resolved vibronic progression (peaks at 461, 428, and 404 nm), which points out a narrower distribution of conjugation lengths as compared to other PPV samples previously studied.[31,32,58–60] The structural order manifested by the long conjugation length and by its narrow distribution is fundamental for isolating the intrinsic optical response of the system from spurious effects. At shorter wavelengths, a shoulder (generally referred to as peak II) is observed around 340 nm in the parallel reflectance.[13–16,39,44,45,54] An additional broad transition (peak III) is manifested around 260 nm in the parallel reflectance. Most of the theoretical studies indicate that peak III originates from a transition between localized and delocalized levels (L-D^* and D-L^*), with a dominant polarization perpendicular to the polymer-chain axis.[44–56] At room temperature, the perpendicular component of peak III is manifested in the perpendicular ($\perp$) reflectance spectrum around 280 nm. Notice that, in order to derive the polarization of this structure from the optical spectra,[13,14,16,61] the contribution from other transitions, such as the one stemming from the π-π^* transition of the parallel component must be properly taken into account.[61] Another transition polarized parallel to the chain axis (not shown here) is known to exist around 200 nm,[16] due to the electron and hole states of a tightly bound Frenkel exciton localized on the phenyl ring (L-L^*);[16,44–56] this transition is responsible for the reflectance increase at the high-energy side of our spectra.

The shape of the reflectance spectra is almost unchanged by lowering the temperature down to 80 K. The spectra appear to be rigidly redshifted by about 10 nm as compared to the corresponding ones at room temperature (0-0 transition and vibronic progression peak at 509, 468, 434, and 408 nm, respectively), indicating an extended conjugation length due to the planarization of the polymer backbone at low temperature. A similar thermal shift has also been observed in high-quality PPV obtained by a different synthetic route.[57]

At long wavelengths, the excellent optical quality of the films is manifested in both the room temperature and the low-temperature reflectance spectra by the interference pattern due to the sum of contributions reflected from the front and the back surfaces of the film. In the reflectance spectra obtained with perpendicular polarization, the onset of absorption, which nullifies the contribution from the back surface, results in an abrupt reduction of the reflectivity intensity around 500 nm. Note that the structure visible at about 800 nm in Fig. 1(a) is an artifact due to the sample holder inside the cryostat; it has been properly normalized during the data reduction to derive the optical constants (see below).

Figure 1 shows also the polarized transmittance of oriented PPV at room temperature [Fig. 1(c)] and 80 K [Fig. 1(d)]. As in reflectance spectra, the appearance of interference fringes testifies the good optical quality of the films. Changes in the interference pattern between the parallel and perpendicular components of transmittance (reflectance) point out to the anisotropy of the refractive index. The optically thick samples used in this work do not allow a direct determination of the transmission spectra below 500 nm, as at these wavelengths the sample is no longer transparent. However, we notice the considerable difference ($\sim$30 nm) in the onset of the transmission for the two polarizations. The thermal shift of the onset of transmission from room temperature to 80 K is about 10 nm (both for parallel and perpendicular polarization), consistent with the bathochromic shift of the reflectance spectra. The lowest optical transition (peak I) has a perpendicular component with respect to the stretching direction that masks the intrinsic absorption.[17] The lowest-energy perpendicular absorption has been attributed to residual chain misalignment in previous studies on oriented polyacetylene and polydiacetylene.[62,63] However, solid-state models that include the effects of crystalline arrangement predict weak transitions with perpendicular polarization as a result of intermolecular interactions.[33]

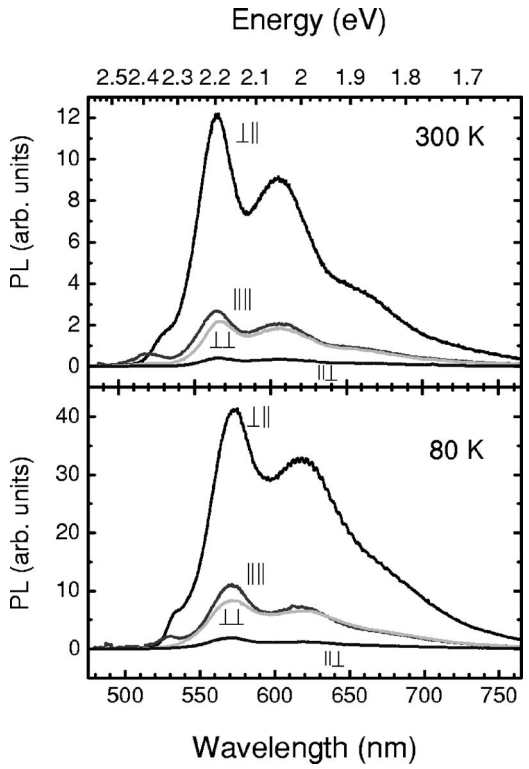

FIG. 2. Polarized PL spectra of highly oriented PPV as obtained exciting the samples at 458 nm at room temperature (upper panel) and 80 K (lower panel). The various configuration of excitation or detection polarizations are indicated in the figure.

B. Photoluminescence

Figure 2 shows the photoluminescence spectra measured in the four configuration of laser excitation or analyzer polarizations at room temperature (upper panel) and 80 K (lower panel). Amongst the four combinations, the ($\perp$,$\parallel$) measurement exhibits the strongest PL intensity; the weakest spectrum is ($\parallel$,$\perp$), while ($\parallel$,$\parallel$) and ($\perp$,$\perp$) have almost the same intensity. At room temperature, peaks at 565 and 605 nm, as well as a shoulder around 660 nm are detected. These emission peaks are redshifted with respect to those previously observed in PPV.[31,32,64] In the ($\perp$,$\parallel$) spectrum, an

additional shoulder can be identified around 530 nm, while the (∥,∥) PL spectrum shows a well-defined peak at 520 nm. The weak high-energy features resemble the 0-0 transitions detected in the PL spectra of thin PPV films;[57,58,65–71] for the remaining polarizations (∥,⊥ and ⊥,⊥) there is no clear evidence for any additional structure underneath the high-energy tail of the main emission peak.

Upon lowering the temperature, the PL signal intensity increases by a factor greater than three and the main spectral peaks slightly shift to longer wavelength (565 nm $\rightarrow$573 nm; 605 nm$\rightarrow$618 nm). Notice that the thermal shift of the main emission peaks is similar to the one of the electronic transitions (both 0-0 and vibronic progression) observed in reflectance spectra, while the shift of the high-energy peaks is larger. Moreover, at low temperature, the relative intensity of the four polarization combinations is almost unchanged, but the high-energy features (at 530–540 nm) are better defined, while the main peaks are unusually broadened compared to room temperature. The anomalous shift of the high-energy bands and their spectral broadening upon lowering the temperature makes their assignment nontrivial: they may originate from different phonons involved in the ground electronic state (probed by PL) and excited electronic state (probed by reflectance), as well as from the influence of intermolecular interactions, as was recently suggested in studies of PPV or silica nanocomposites[31,32] and MEH-PPV films cast from different solvents.[30,72]

For a better understanding of the origin of the emission peaks it is essential to correct the emission spectra for an equal number of absorbed (exciting) photons, as well as for self-absorption and reflectivity losses. Considering the strong anisotropy of the optical properties and their different spectral dispersion, noticeable effects due to these corrections are expected both for spectral shapes and emission intensities in the various polarization configurations. The dispersion of the refractive index (n) and absorption coefficient (k) and their dependence on polarization would strongly affect the emission spectra, particularly in the spectral region overlapped with the high-energy emission peaks.

C. Determination of the optical constants

Many methods are known for the determination of the optical constants.[2–4,73,74] In order to deduce the anisotropic complex dielectric constants of PPV at different temperatures, we have employed the combination of two complementary methods, namely, the Kramers-Kronig analysis of reflectivity over the whole spectral range,[16] and an interferometric method in the transparent spectral region (where $k=0$). This interferometric method, based on a Mach-Zehnder interferometer coupled with a commercial scanning Michelson interferometer (SMI), has been described in details in a previous publication.[75] As opposed to other conventional techniques for the determination of the refractive index,[37] this method allows for the direct and simultaneous determination of the refractive index and polymer film thickness ($d=15.1$ μm) even in the case of anisotropic samples. Thanks to the high stability and reproducibility of the commercial SMI, the uncertainty in the determination of both n and d is estimated to be less than 0.6% of their values.[75] The dispersion curves determined by the white-light interferometric technique in the transparent region provide a starting point and a quality check for the Kramers-Kronig analysis of the absolute reflectivity, by which the determination of the optical-constants dispersion can be extended also to the absorbing region (where $k\neq 0$).

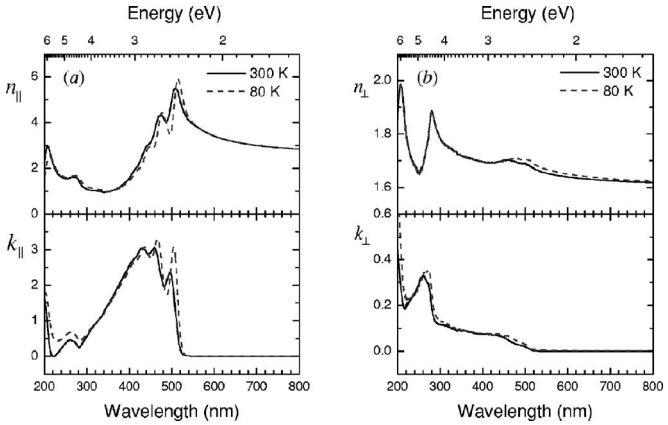

FIG. 3. Frequency dispersion of the parallel (a) and perpendicular (b) components of the real part (upper panels) and the imaginary part (lower panels) of the refractive index of PPV as determined at room temperature (solid lines) and $T=80$ K (dashed lines).

Figure 3 shows the real and the imaginary components of the refractive index in the parallel (left panel) and perpendicular (right panel) direction with respect to the polymer chain axis, as determined at room temperature (solid lines) and 80 K (dashed lines). The corresponding components of the dielectric constant can be easily derived as $\varepsilon_1=n^2-k^2$ and $\varepsilon_2=2nk$. For comparison with the reflectivity obtained with the automatic spectrophotometer (which includes interference effects), the bulk reflectivity spectrum calculated from the optical constants for parallel polarization is also shown in Fig. 1(a) (dotted line).

The exceedingly high anisotropy of the oriented PPV samples can be properly evaluated by the dichroic ratio of the dielectric constant ($\varepsilon_2^{\parallel}/\varepsilon_2^{\perp}\sim 300$ at 500 nm). The use of ε_2 instead of k (or the absorption coefficient) is preferable since the imaginary part of the dielectric constant is directly related to the electronic structure of a semiconductor.[76] The intrinsic ⊥ components of the dielectric functions are masked by a slight misalignment of the chain orientation around the stretching direction. This misalignment induces an apparent ⊥ component of the dipole-transition moment due to the projection of the ∥ component that scales as $\sin^2\theta/2$, θ being the misalignment angle.[62] The feature around 500 nm in $\varepsilon_2^{\perp}$, for example, is mainly a manifestation of the perpendicular component of peak I, due to the residual chain misalignment. From the conventional expression of the orientation function r $[r=(I_{\parallel}-I_{\perp})/(I_{\parallel}+2I_{\perp})$, where $I_{\parallel}=I\cos^2\vartheta$ and $I_{\perp}=(I\sin^2\vartheta)/2$ are the parallel and perpendicular components of the optical function $I]$[23,77] we obtain $r=0.99$ at 500 nm for the low-temperature curves, which corresponds to an average misalignment angle smaller than $\theta=5°$.

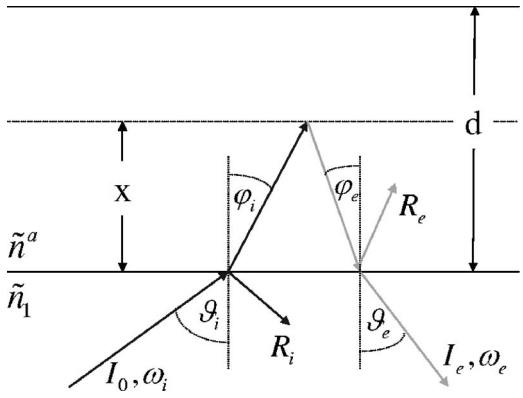

FIG. 4. Scheme of photoexcitation and emitted PL optical paths used to correct the PL spectra.

D. Correction of the photoluminescence spectra

1. Modeling the anisotropic absorption and refractive effects on the external photoluminescence

The large optical anisotropy of highly oriented polymer films requires drastic corrections to be applied to the measured photoluminescence spectra. In order to do so, we will treat the oriented PPV films as uniaxial materials with optical axis parallel to the drawing direction. This assumption is justified by the cylindrical symmetry induced by the stretching procedure. Figure 4 is a schematic representation of the typical configuration in which photoluminescence experiments are carried out, where the polymer film with refractive index $\tilde{n}^a$ and thickness d is surrounded by a medium (air) with index $\tilde{n}_1$. The incident excitation beam, of intensity I_0 and frequency ω_i, is directed to the polymer surface at an angle ϑ_i, being partially reflected and refracted at the interface. If we assume the optical axis of the oriented film to be perpendicular to the plane of incidence, the exciting beam will be refracted at an angle φ_i according to Snell's law:

$$\tilde{n}_1(\omega_i)\sin\,\vartheta_i = \tilde{n}^{a_i}(\omega_i)\sin\,\varphi_i, \tag{1}$$

where the polarization of the incident beam a_i can be either parallel ($a_i = \parallel$) or perpendicular ($a_i = \perp$) to the optical axis. The portion of the beam that penetrates into the film is absorbed according to the generalized Lambert-Beer law for oblique incidence (for air, $k_1 = 0$):[78]

$$I^a = I_0 \exp(-A^a x), \tag{2}$$

where A is

$$A^a(\omega,\vartheta) = \frac{2\omega}{c}\,\mathrm{Im}(\sqrt{(\tilde{n}^a)^2 - (n_1\,\sin\,\vartheta)^2}) = \frac{2\omega}{c}\,\mathrm{Im}(N^a + iK^a) = \frac{2\omega K^a}{c}. \tag{3}$$

The expressions for N^a and K^a are given by Eq. (A3) in the Appendix. The amplitude attenuation depends only on the penetration depth x, and constant amplitude planes are parallel to the boundary surface that separates the environment from the absorbing medium. For each x the absorbed light results in a photoluminescence spectrum emitted according to the intensity distribution of the emitting dipoles. On its way back to the front surface, photoluminescence is partially reabsorbed by the polymer (self-absorption). Then, after being partially reflected at the interface, only the beams that are refracted at the detection angle ϑ_e will contribute to the measured PL intensity I_e, emitted at frequency ω_e. Again, the outgoing beams with incidence angle φ_e will be refracted from the inside out according to Snell's law,

$$\tilde{n}^{a_e}(\omega_e)\sin\,\varphi_e = \tilde{n}_1(\omega_e)\sin\,\vartheta_e, \tag{4}$$

where the polarization of the emitted beam a_e can be either parallel ($a_e = \parallel$) or perpendicular ($a_e = \perp$) to the polymer optical axis. Note that the contributions of those beams that are reflected by the back polymer surface and then refracted at the detection angle have been neglected. This approach is justified by the very weak amplitude detected for the interference fringes observed in the PL spectra [Fig. 2, low temperature ($\perp$, $\parallel$) and ($\parallel$, $\parallel$) configurations only]. Under these conditions, the observed photoluminescence intensity $I_e^{a_i,a_e}(\omega_e)$ for the four possible configurations of excitation and detection polarizations (a_i, a_e) can be written as

$$I_e^{a_i,a_e}(\omega_e) = I_0^{a_i}(\omega_i)\,\eta^{a_i}(\omega_i)C[1 - R_i^{a_i}(\omega_i,\vartheta_i)]A_i^{a_i}(\omega_i,\vartheta_i) \times \int_0^d dx e^{-A_i^{a_i}(\omega_i,\vartheta_i)x}\mathrm{PL}^{a_i,a_e}(\omega_e)e^{-A_e^{a_e}(\omega_e,\vartheta_e)x} \times [1 - R_e^{a_e}(\omega_e,\vartheta_e)], \tag{5}$$

where $\mathrm{PL}_{ie}^{a,a}$ is the intrinsic emission spectrum, η is the internal quantum efficiency, C is a geometrical factor, and $R_i^{a_i}, R_e^{a_e}$ are the reflectance coefficients given by Eq. (A5) in the Appendix. A similar approach has been previously adopted for the determination of the Raman cross sections of oriented polymer films.[79] The main difference between PL and Raman spectral corrections, however, is that the former are related to incoherent processes, while the latter to a coherent one. Equation (5) can be rewritten as

$$I_e^{a_i,a_e}(\omega_e) = I_0^{a_i}(\omega_i)\,\eta^{a_i}(\omega_i)C[1 - R_i^{a_i}(\omega_i,\vartheta_i)]\mathrm{PL}^{a_i,a_e}(\omega_e) \times [1 - R_e^{a_e}(\omega_e,\vartheta_e)]F^{a_i,a_e}, \tag{6}$$

with

$$F^{a_i,a_e} = A_i^{a_i}(\omega_i,\vartheta_i)\int_0^d dx e^{-[A_i^{a_i}(\omega_i,\vartheta_i)+A_e^{a_e}(\omega_e,\vartheta_e)]x} = \frac{A_i^{a_i}(\omega_i,\vartheta_i)(1 - e^{-[A_i^{a_i}(\omega_i,\vartheta_i)+A_e^{a_e}(\omega_e,\vartheta_e)]d})}{A_i^{a_i}(\omega_i,\vartheta_i) + A_e^{a_e}(\omega_e,\vartheta_e)}. \tag{7}$$

Therefore, the intrinsic emission spectra can be obtained normalizing the observed photoluminescence spectra according to

$$\mathrm{PL}^{a_i,a_e}(\omega_e) = \frac{1}{\eta^{a_i}(\omega_i)C}\frac{I_e^{a_i,a_e}(\omega_e)}{I_0^{a_i}(\omega_i)}Q^{a_i,a_e}(\omega_i,\omega_e,\vartheta_i,\vartheta_e). \tag{8}$$

The first factor on the right-hand side of Eq. (8) contains all the constants, and the correction factors Q^{a_i,a_e} are given by

$$Q^{a_i,a_e}(\omega_i,\omega_e,\vartheta_i,\vartheta_e)=\frac{A_i^{a_i}(\omega_i,\vartheta_i)+A_e^{a_e}(\omega_e,\vartheta_e)}{A_i^{a_i}(\omega_i,\vartheta_i)[1-R_i^{a_i}(\omega_i,\vartheta_i)][1-R_e^{a_e}(\omega_e,\vartheta_e)](1-e^{-[A_i^{a_i}(\omega_i,\vartheta_i)+A_e^{a_e}(\omega_e,\vartheta_e)]d})}. \quad (9)$$

Q are the factors the measured PL spectra must be multiplied for, in order to account for self-absorption and refractive effects, namely, partial reflection of the exciting beam from the polymer surface and self-absorption and reflection of the emitted PL on its way out of the polymer film. The evaluation of these factors requires the knowledge of the optical constants (ε_1 and ε_2) dispersion, both in the absorption and emission spectral region.

2. The case of oriented PPV

Figure 5 shows the PL spectra of oriented PPV films corrected according to Eqs. (8) and (9) for the various configurations of the excitation or detection polarizations at room temperature [Figs. 5(a) and 5(b)] and $T=80$ K [Figs. 5(c) and 5(d)]. The corrections modify the spectral shape of the PL as well as the relative magnitude of the PL peak intensities. Due to the highly anisotropic optical properties of oriented PPV, the correction factors are strongly dependent on the experimental configuration of the polarizations and are more relevant where the dispersion of the refractive index is high, e.g., on the high-energy side of the PL spectra. The low-energy side of the corrections is weakly dispersive and, since the sample is transparent in this region, it is mainly due to the different reflectivity in each given configuration of the polarizations. For instance, the largest correction corresponds to the (∥,∥) configuration, where the emission suffers the highest losses due to the high reflection of the excitation as well as of the emission at the polymer-air interface, while the smallest correction applies to the (⊥,⊥) configuration where reflection of both excitation and emission is lower. Remarkably, in the high-energy region (wavelengths around 520–530 nm), the two features seen in the (⊥,∥) and (∥,∥) configurations prior to the correction (Fig. 2) merge into a single peak centered at 517 nm at room temperature (530 nm at 80 K). In spite of the correction, the (⊥,∥) and (⊥,⊥) components of the emission remain more intense than the (∥,∥) and (∥,⊥) components, respectively [Figs. 5(a) and 5(c) and Figs. 5(b) and 5(d)], although their difference is significantly reduced.

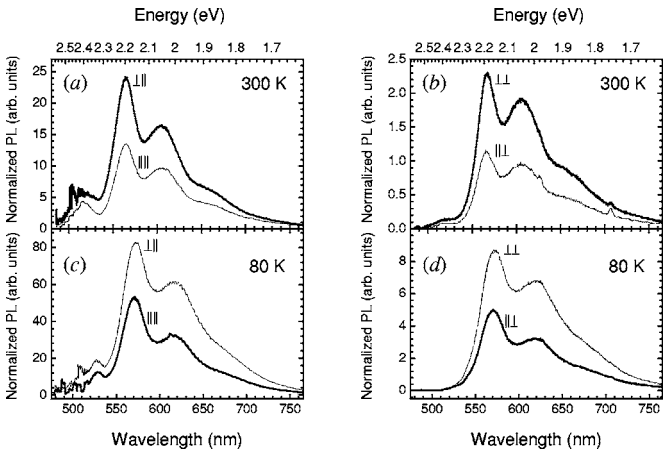

FIG. 5. Polarized PL spectra of highly oriented PPV at room temperature [(a) and (b)] and 80 K [(c) and (d)] corrected for self-absorption and refractive effects.

3. Refractive-index effects on photon emission and extraction

The corrections applied to the emission spectra so far (Fig. 5) account for the anisotropy of light penetration or absorption of both the excitation beam and the light emitted through the sample surface. As pointed out in the Introduction, the refractive index further affects the photoluminescence efficiency by influencing the internal emission rate through the phase propagation of the emitted light in the medium surrounding the emitters and through local-field effects, as well as the external emission rate by affecting the light extraction from the polymer film. In the following we will discuss these two additional effects of the refractive index on the photoluminescence of anisotropic systems.

The intensity of spontaneous emission is proportional to the number of molecules in the excited state and to their transition-dipole moments:[80] the power of the radiation emitted by an electric dipole is proportional to n^3 (which accounts for the phase propagation of the emitted wave in the medium surrounding the emitter),[81,82] and is inversely proportional to the dielectric function ε (which accounts for local-field effects in isotropic systems).[82] In the transparent region, where $\varepsilon=n^2$, the emission probability is therefore proportional to the refractive index n.[83] Note that such a dependence of the emission probability on the refractive index is valid only for an isotropic system. To the best of our knowledge, a comprehensive theory for local-field effects on the emission properties of anisotropic organic systems has not yet been developed. Therefore, for a qualitative evaluation of the spontaneous emission rate in oriented PPV, we will assume the isotropic model to be applicable to each individual polarization component of the PL.

An additional effect of the refractive index on polarized emission spectra concerns light extraction from the anisotropic polymer film, as widely discussed in the literature of organic light emitting diodes.[36,38] Since PL measurements are usually performed by collecting a cone of light with finite numerical aperture, only a portion of the solid angle at which light is emitted can be collected. The fraction of emitted light that is collected is related to the refractive index by Snell's law, thus, in anisotropic media, it depends on the beam polarization.[84] An estimate of such an effect can be obtained by differentiating Snell's law with respect to the collection angle ($\delta\alpha$) and considering the solid angle as proportional to $\delta\alpha^2$. Doing so, one obtains a ratio between the internal sector

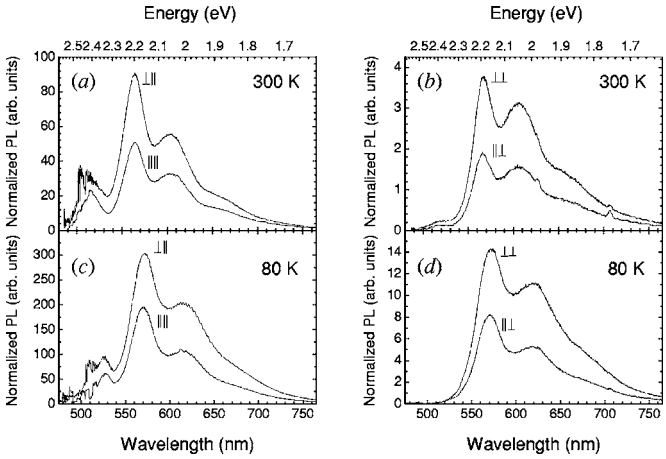

FIG. 6. Polarized PL spectra of highly oriented PPV at room temperature [(a) and (b)] and 80 K [(c) and (d)] obtained using the final correction functional expression presented in Sec. III D 3.

of solid angle and the external one of $[1-\sin^2(\alpha)]/[n^2-\sin^2(\alpha)]$.[36,85] In oriented PPV, since $n\| \gg n\perp$, the light cone collected with polarization parallel to the polymer chain axis probes a much smaller fraction of emitted light (and thus the collected PL signal appears weaker) than the same light cone collected with polarization perpendicular to the polymer chain axis. For each polarization, the spectral dependence of the PL on the refractive index due to light extraction is proportional to $1/n^2$.

In order to account for the combination of these two effects of the refractive index, one can multiply the spectra in Fig. 5 by the refractive index n corresponding to the emission polarization (Fig. 6). Qualitatively (local-field effects in anisotropic systems are hereby neglected), the effect of this correction is to enhance the emission anisotropy and to increase the relative intensity of the high-energy structure as compared to the main emission peaks.

E. Excitation and emission anisotropy

After the correction of the emission spectra according to the complex procedure described above, it is evident that PL spectra of oriented PPV show both excitation and emission anisotropy.

1. Excitation anisotropy (pump polarization anisotropy)

The intensity of the PL spectra derived from excitation polarized perpendicular to the draw axis results in PL almost twice as strong compared to the PL derived for excitation polarized parallel to the draw axis, independently on the polarization of the emission. A similar intensity ratio (often referred to as pump polarization anisotropy) has been previously observed in the photoinduced absorption due to charged states in polydiacetylene[63] and in photoconductivity measurements of oriented polyacetylene[62] and PPV.[86] This could be understood in terms of charged carrier-induced exciton quenching,[87–89] as indeed is supported by the high-charge photogeneration efficiency,[90–92] the lack of stimulated emission in PA measurements,[93] and the relatively low PL quantum efficiency measured in these films (see below). For $\|$ polarization, the small absorption depth ($\sim$12 nm) results in a rather high concentration of excitons and carriers near the sample surface of both, relatively short-lived free carriers and long-lived ones that are localized at trap sites, which increases the probability of carrier-induced exciton quenching. On the other hand, for $\perp$ polarization the light-penetration depth is significantly enhanced (by a factor of $\sim$100) and thus the probability for charged carrier-induced exciton quenching is strongly reduced. Note that pump polarization anisotropy has been generally observed in optically thick samples[94] since in thin samples, as those obtained by blending conjugated polymers with ultrahigh molecular-weight polyethylene[25–28] or by rubbing thin polymer films,[29] the excitation volume coincides with the entire sample volume and therefore is independent on pump polarization.

Time-resolved photoluminescence measurements probing the emission at 557 nm in the nanosecond time range have shown for both of the emission polarizations a faster PL decay with excitation parallel to the draw axis compared with excitation perpendicular to the draw axis. A similar anisotropy of the charge-carrier lifetimes has been observed in fast transient photoconductivity measurements of oriented PPV, lifetimes which are also much longer than the singlet excitons lifetime;[95] this behavior is consistent with charge-exciton quenching affecting the exciton relaxation dynamics. Charge-exciton quenching is expected to depend also on the excitation intensity, which affects carrier and exciton density as well as bimolecular recombination processes (both carrier-carrier and exciton-exciton).

The external quantum efficiency (QE) values we have determined for highly oriented PPV by an integrating sphere are quite low compared to the QE measured in conventional soluble PPV derivatives, where QEs as high as 27% have been previously found. In agreement with the polarization anisotropy deduced from the spectra in Fig. 5, the external QE measured with excitation polarized perpendicular to the draw axis (4.7%) is about twice the QE measured with parallel polarization of the excitation (2.2%). Since the low-excitation intensity employed in these measurements rules out bimolecular effects (self-quenching), this further supports our hypothesis of charge-carrier-induced exciton quenching. Enhanced oxidation at the sample surface could also explain the above observations, however, IR transmission measurements (both with standard and photoacoustic detection) have shown the lack of any signal associated with carbonyl groups. This indicates a very low density of carbonyl groups (below the sensitivity of our measuring systems) in these samples and therefore rules out oxidation as the reason for the pump polarization anisotropy and the low PL external QE observed.

2. Emission polarization anisotropy

In order to discuss the emission polarization anisotropy (for a given pump polarization) it is instructive to plot the orientation function r relative to the PL spectra corrected for all the effects discussed so far. Figure 7 shows the orientation functions derived from the spectra in Fig. 6.

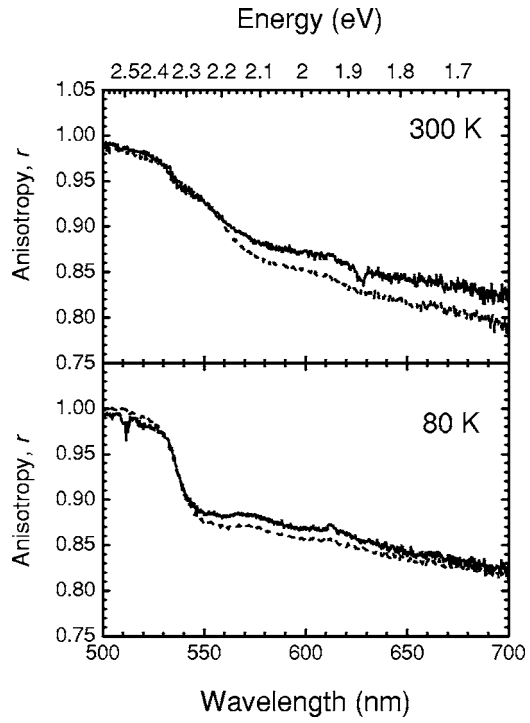

FIG. 7. Spectral dependence of the emission orientation function (anisotropy, r) for parallel (solid curves) and perpendicular (dashed curves) polarization of the excitation. Upper panel: room temperature; lower panel: $T=80$ K.

As expected, the anisotropy is almost independent of the excitation route; however, a strong spectral dependence of the anisotropy functions is evident, in particular, at low temperature, with almost complete polarization of the high-energy emission peak along the polymer chain axis ($r>0.99$), and considerably lower polarization of the low-energy structures ($r\sim0.85$). Note that neglecting local-field effects[31,32] would lead to underestimating the anisotropy at low energies, and would enhance the spectral dispersion of r.

The dependence of the orientation function on the emission wavelength, with crossover at about 540 nm, suggests a different origin of the emitting states responsible for the high-energy (520–530 nm) and the low-energy peaks of the photoluminescence. This conclusion is further supported by the different temperature dependence of the high- and low-energy PL peaks (Fig. 2). The existence of more than a single emitting state could be understood in different ways. One explanation is to assume a bimodal distribution of conjugation length, as previously proposed for the interpretation of the optical properties of disordered PPV.[64,66,96] However, the sharp optical transitions observed in the reflectance spectra of our samples are inconsistent with this interpretation. Another possible explanation may be the presence of defects acting as a sink for the excitations and providing an alternative excitation deactivation pathway to the standard intramolecular radiative decay. Energy transfer[97] can explain the strong intensity of the low-energy part of the PL spectrum of highly ordered PPV, as well as its unusually large ($\sim$0.2 eV) apparent Stokes shift. The high-energy part of the PL spectrum, with intrinsic anisotropy comparable to that of the absorption, could be assigned to an intramolecular decay, while the low-energy one to a "defect." The role of defects on the emission properties of organic semiconductors has been previously elucidated for oligothiophene single crystals.[98]

In our case, the origin of such defects may be related to the morphology of the PPV films. These films are composed of crystalline regions (70% of the volume) and amorphous regions.[99] Within each crystallite ($\sim$20 nm size), chains are packed in an orthorhombic structure with intermolecular separations of either 5 Å (translational periodicity along the b axis) or 3.9 Å (between benzene ring layers inside the unit cell). Even though the highest interchain coupling is predicted to take place in the cofacial arrangement, such intermolecular separations can allow significant intermolecular interactions.[100] Thus, the two emitting states we observe may be correlated with the amorphous and crystalline phases coexisting in the oriented PPV samples. In the amorphous phase, the electronic transitions mainly stem from isolated macromolecules (emitting at higher energies, possibly due to the shorter localization length). In contrast, in the crystalline phase intermolecular interactions would affect the electronic structure[15] that should be described using solid-state models that include the effects of crystalline arrangement, models that predict weak transitions with perpendicular polarization,[33] as well as reduce the energy gap and lower the emission energy.[101,102] Note that the reduced anisotropy cannot be attributed to chain misalignment, as $r=0.85$ corresponds to a misalignment angle much higher than the one derived from reflectance measurements ($r=0.99$).

Intermolecular interactions have been previously proposed for the interpretation of the emission properties of PPV-silica nanoparticles composites (where the high-energy emission would stem from a molecular state while the low-energy emission would stem from molecular aggregates),[31,32] of other PPV derivatives[30,103–105] and of poly(p-phenylene ethynylenes).[106] All our findings suggest that, in the crystalline phase, the mechanism of exciton quenching by charged polarons may be very efficient. Moreover, due to the high degree of order and crystallinity of our samples a dark state originating from strong interchain interactions may also be present in the HOMO-LUMO gap,[33] thus reducing significantly the luminescence yield.

IV. CONCLUSIONS

We have presented a detailed characterization of the polarized optical and emission properties of highly oriented PPV samples at various temperatures, derived from the analysis of polarized transmission, reflectance, and PL spectra. The anisotropic complex refractive index of highly oriented PPV at room temperature and 80 K has been derived. The analysis of the data requires corrections due to PL self-absorption and refractive losses in the various configurations of the polarizations as well as to the influence of the refractive index dispersion on the emission rate and on light extraction from the polymer film. We have developed an analytical model for the excitation or emission of a uniaxial slab and evaluated the effect of highly dispersive anisotropic op-

tical functions on the polarized emission. From the corrected spectra we have derived the excitation and emission anisotropy of highly oriented PPV: the pump polarization anisotropy has been attributed to charge-induced luminescence quenching while the spectral dependence of the emission anisotropy suggests the existence of different states emitting at higher and lower energies. The high-energy part of the PL spectrum (below 540 nm), is fully polarized along the stretching direction and is assigned to an intramolecular excited state. The low-energy part of the PL spectrum (above 540 nm) shows reduced anisotropy, possibly due to intermolecular interactions.

ACKNOWLEDGMENTS

We are grateful to A. J. Heeger for his support and for the useful discussions regarding this paper. We thank A. Mikhailovsky for his help in the photoluminescence measurements. C.S. acknowledges the support of D. Wang during the preparation of the manuscript. This work was supported by the National Science Foundation under Grants No. DMR-0099843 and No. DMR-0096820, and by the Italian Ministry of Instruction, University and Research (MIUR) under the project "Synergy," FIRB 2003.

APPENDIX: REFLECTIVITY FROM ANISOTROPIC UNIAXIAL MEDIA

Let us consider a light beam traveling in air ($\tilde{n}_1=1$) and illuminating the oriented polymer film with the plane of incidence perpendicular to the principal optical axis. Due to this specific geometrical configuration (configuration that we have utilized for polarized photoluminescence measurements in oriented PPV), the p component of the electric field (parallel to the plane of incidence) is affected only by the ordinary dielectric constant, while the s component of the electric field (perpendicular to the plane of incidence) is affected only by the extraordinary dielectric constant. Therefore, the usual expression[78] for the p and s components of the reflection coefficient, $\tilde{r}_p$ and $\tilde{r}_s$, becomes

$$\tilde{r}_p = \frac{(\tilde{n}^{\perp})^2 \cos\vartheta - \sqrt{(\tilde{n}^{\perp})^2 - \sin^2\vartheta}}{(\tilde{n}^{\perp})^2 \cos\vartheta + \sqrt{(\tilde{n}^{\perp})^2 - \sin^2\vartheta}} = \frac{(\varepsilon_1^{\perp} + i\varepsilon_2^{\perp})\cos\vartheta - \sqrt{(\varepsilon_1^{\perp} - \sin^2\vartheta) + i\varepsilon_2^{\perp}}}{(\varepsilon_1^{\perp} + i\varepsilon_2^{\perp})\cos\vartheta + \sqrt{(\varepsilon_1^{\perp} - \sin^2\vartheta) + i\varepsilon_2^{\perp}}},$$

$$\tilde{r}_s = \frac{\cos\vartheta - \sqrt{(\tilde{n}^{\parallel})^2 \sin^2\vartheta}}{\cos\vartheta + \sqrt{(\tilde{n}^{\parallel})^2 - \sin^2\vartheta}} = \frac{\cos\vartheta - \sqrt{(\varepsilon_1^{\parallel} - \sin^2\vartheta) + i\varepsilon_2^{\parallel}}}{\cos\vartheta + \sqrt{(\varepsilon_1^{\parallel} - \sin^2\vartheta) + i\varepsilon_2^{\parallel}}}. \tag{A1}$$

If we define N^a and K^a, where $a=\parallel$ or $\perp$, such as

$$\sqrt{(\varepsilon_1^a - \sin^2\vartheta) + i\varepsilon_2^a} = N^a + iK^a, \tag{A2}$$

it is straightforward to show that

$$N^a = \sqrt{\frac{\sqrt{[\varepsilon_1^a - (n_1\sin\vartheta)^2]^2 + (\varepsilon_2^a)^2} + \varepsilon_1^a - (n_1\sin\vartheta)^2}{2}},$$

$$K^a = \sqrt{\frac{\sqrt{[\varepsilon_1^a - (n_1\sin\vartheta)^2]^2 + (\varepsilon_2^a)^2} - \varepsilon_1^a + (n_1\sin\vartheta)^2}{2}}, \tag{A3}$$

and

$$\tilde{r}_p = \frac{(\varepsilon_1^{\perp}\cos\vartheta - N^{\perp}) + i(\varepsilon_2^{\perp}\cos\vartheta - K^{\perp})}{(\varepsilon_1^{\perp}\cos\vartheta + N^{\perp}) + i(\varepsilon_2^{\perp}\cos\vartheta + K^{\perp})},$$

$$\tilde{r}_s = \frac{(\cos\vartheta - N^{\parallel}) - iK^{\parallel}}{(\cos\vartheta + N^{\parallel}) + iK^{\parallel}}. \tag{A4}$$

Using Eqs. (A3) and (A4) one can finally express the parallel and perpendicular reflectance in terms of the ordinary and extraordinary components of the dielectric functions

$$R^{\parallel}(\omega,\vartheta) = |\tilde{r}_s|^2 = \frac{(\cos\vartheta - N^{\parallel})^2 + (K^{\parallel})^2}{(\cos\vartheta + N^{\parallel})^2 + (K^{\parallel})^2},$$

$$R^{\perp}(\omega,\vartheta) = |\tilde{r}_p|^2 = \frac{(\varepsilon_1^{\perp}\cos\vartheta - N^{\perp})^2 + (\varepsilon_2^{\perp}\cos\vartheta - K^{\perp})^2}{(\varepsilon_1^{\perp}\cos\vartheta + N^{\perp})^2 + (\varepsilon_2^{\perp}\cos\vartheta + K^{\perp})^2}. \tag{A5}$$

In the case of the light beam traveling from the inside out of the uniaxial slab, Eq. (A5) still holds if ϑ denotes the refraction angle.

*Corresponding author. Present address: Department of Electrical and Computer Engineering, University of California, San Diego. Email address: csoci@ece.ucsd.edu

[1] *Supramolecular Polymers* (Taylor & Francis, Boca Raton, 2005).
[2] M. Tammer and A. P. Monkman, Adv. Mater. (Weinheim, Ger.) **14**, 210 (2002).
[3] C. M. Ramsdale and N. C. Greenham, Adv. Mater. (Weinheim, Ger.) **14**, 212 (2002).
[4] D. Comoretto and G. Lanzani, in *Organic Photovoltaic*, edited by C. J. Brabec, V. Dyakonov, J. Parisi, and S. N. Sariciftci (Springer, Berlin, 2003).
[5] K. Akagi, M. Suezaki, H. Shirakawa, H. Kyotani, M. Shimomura, and Y. Tanabe, Synth. Met. **28**, D1 (1989).
[6] S. Z. Tokito, P. Smith, and A. J. Heeger, Synth. Met. **36**, 183 (1990).
[7] S. Tokito, P. Smith, and A. J. Heeger, Polymer **32**, 464 (1991).
[8] D. D. C. Bradley, J. Phys. D **20**, 1389 (1987).
[9] A. Bolognesi, C. Botta, D. Facchinetti, M. Jandke, K. Kreger, P.

Strohriegl, A. Relini, R. Rolandi, and S. Blumstengel, Adv. Mater. (Weinheim, Ger.) **13**, 1072 (2001).
[10] T. Virgili, D. G. Lidzey, M. Grell, S. Walker, A. Asimakis, and D. D. C. Bradley, Chem. Phys. Lett. **341**, 219 (2001).
[11] J. H. Burroughes, D. D. C. Bradley, A. R. Brown, R. N. Marks, K. Mackay, R. H. Friend, P. L. Burns, and A. B. Holmes, Nature (London) **347**, 539 (1990).
[12] D. Braun and A. J. Heeger, Appl. Phys. Lett. **58**, 1982 (1991).
[13] E. K. Miller, D. Yoshida, C. Y. Yang, and A. J. Heeger, Phys. Rev. B **59**, 4661 (1999).
[14] E. K. Miller, C. Y. Yang, and A. J. Heeger, Phys. Rev. B **62**, 6889 (2000).
[15] E. K. Miller, G. S. Maskel, C. Y. Yang, and A. J. Heeger, Phys. Rev. B **60**, 8028 (1999).
[16] D. Comoretto, G. Dellepiane, F. Marabelli, J. Cornil, D. A. dos Santos, J. L. Bredas, and D. Moses, Phys. Rev. B **62**, 10173 (2000).
[17] D. Moses, J. Wang, A. J. Heeger, N. Kirova, and S. Brazovski, Proc. Natl. Acad. Sci. U.S.A. **98**, 13496 (2001).
[18] M. Losurdo, G. Bruno, and E. A. Irene, J. Appl. Phys. **94**, 4923 (2003).
[19] G. Leising, Phys. Rev. B **38**, 10313 (1988).
[20] D. D. C. Bradley, Y. Q. Shen, H. Bleier, and S. Roth, J. Phys. C **21**, L515 (1988).
[21] M. Grell and D. D. C. Bradley, Adv. Mater. (Weinheim, Ger.) **11**, 895 (1999).
[22] T. Virgili, D. G. Lidzey, M. Grell, D. D. C. Bradley, S. Stagira, M. Zavelani-Rossi, and S. De Silvestri, Appl. Phys. Lett. **80**, 4088 (2002).
[23] H. M. Liem, P. Etchegoin, K. S. Whitehead, and D. D. C. Bradley, Adv. Funct. Mater. **13**, 66 (2003).
[24] K. Pichler, R. H. Friend, P. L. Burn, and A. B. Holmes, Synth. Met. **55**, 454 (1993).
[25] T. W. Hagler, K. Pakbaz, J. Moulton, F. Wudl, P. Smith, and A. J. Heeger, Polym. Commun. **32**, 339 (1991).
[26] T. W. Hagler, K. Pakbaz, K. F. Voss, and A. J. Heeger, Phys. Rev. B **44**, 8652 (1991).
[27] T. W. Hagler, K. Pakbaz, and A. J. Heeger, Phys. Rev. B **49**, 10968 (1994).
[28] S. Luzzati, I. Moggio, D. Comoretto, C. Cuniberti, and G. Dellepiane, Synth. Met. **95**, 47 (1998).
[29] L. M. Herz and R. T. Phillips, Phys. Rev. B **61**, 13691 (2000).
[30] T. Q. Nguyen, R. C. Kwong, M. E. Thompson, and B. J. Schwartz, Appl. Phys. Lett. **76**, 2454 (2000).
[31] P. K. H. Ho, J. S. Kim, N. Tessler, and R. H. Friend, J. Chem. Phys. **115**, 2709 (2001).
[32] P. K. H. Ho and R. H. Friend, J. Chem. Phys. **116**, 6782 (2002).
[33] A. Ruini, M. J. Caldas, G. Bussi, and E. Molinari, Phys. Rev. Lett. **88**, 206403 (2002).
[34] T. G. Pedersen, Phys. Rev. B **69**, 075207 (2004).
[35] I. D. W. Samuel, G. Rumbles, and C. J. Collison, Phys. Rev. B **52**, 11573 (1995).
[36] J. S. Kim, P. K. H. Ho, N. C. Greenham, and R. H. Friend, J. Appl. Phys. **88**, 1073 (2000).
[37] M. Campoy-Quiles, P. G. Etchegoin, and D. D. C. Bradley, Phys. Rev. B **72**, 045209 (2005).
[38] W. M. V. Wan, N. C. Greenham, and R. H. Friend, J. Appl. Phys. **87**, 2542 (2000).
[39] D. Comoretto, G. Dellepiane, D. Moses, J. Cornil, D. A. dos Santos, and J. L. Bredas, Chem. Phys. Lett. **289**, 1 (1998).
[40] T. Ohnishi, T. Noguchi, T. Nakano, M. Hirooka, and I. Murase, Synth. Met. **41**, 309 (1991).
[41] S. Kuroda, T. Noguchi, and T. Ohnishi, Phys. Rev. Lett. **72**, 286 (1994).
[42] S. Doi, M. Kuwabara, T. Noguchi, and T. Ohnishi, Synth. Met. **57**, 4174 (1993).
[43] N. C. Greenham, I. D. W. Samuel, G. R. Hayes, R. T. Phillips, Y. A. R. R. Kessener, S. C. Moratti, A. B. Holmes, and R. H. Friend, Chem. Phys. Lett. **241**, 89 (1995).
[44] N. Kirova, S. Brazovskii, and A. R. Bishop, Synth. Met. **100**, 29 (1999).
[45] S. Brazovskii, N. Kirova, A. R. Bishop, V. Klimov, D. McBranch, N. N. Barashkov, and J. P. Ferraris, Opt. Mater. (Amsterdam, Neth.) **9**, 472 (1998).
[46] A. Kohler, D. A. dos Santos, D. Beljonne, Z. Shuai, J. L. Bredas, A. B. Holmes, A. Kraus, K. Mullen, and R. H. Friend, Nature (London) **392**, 903 (1998).
[47] M. Chandross, S. Mazumdar, M. Liess, P. A. Lane, Z. V. Vardeny, M. Hamaguchi, and K. Yoshino, Phys. Rev. B **55**, 1486 (1997).
[48] M. Chandross and S. Mazumdar, Phys. Rev. B **55**, 1497 (1997).
[49] Y. Shimoi and S. Abe, Synth. Met. **78**, 219 (1996).
[50] J. Cornil, D. A. dos Santos, D. Beljonne, and J. L. Bredas, J. Phys.: Condens. Matter **99**, 5604 (1995).
[51] M. Fahlman, M. Logdlund, S. Stafstrom, W. R. Salaneck, R. H. Friend, P. L. Burn, A. B. Holmes, K. Kaeriyama, Y. Sonoda, O. Lhost, F. Meyers, and J. L. Bredas, Macromolecules **28**, 1959 (1995).
[52] Y. N. Gartstein, M. J. Rice, and E. M. Conwell, Phys. Rev. B **51**, 5546 (1995).
[53] Y. N. Gartstein, M. J. Rice, and E. M. Conwell, Phys. Rev. B **52**, 1683 (1995).
[54] J. Cornil, D. Beljonne, R. H. Friend, and J. L. Bredas, Chem. Phys. Lett. **223**, 82 (1994).
[55] J. Cornil, D. Beljonne, Z. Shuai, T. W. Hagler, I. Campbell, D. D. C. Bradley, J. L. Bredas, C. W. Spangler, and K. Mullen, Chem. Phys. Lett. **247**, 425 (1995).
[56] C. Ambrosch-Draxl and R. Abt, Synth. Met. **85**, 1099 (1997).
[57] K. Pichler, D. A. Halliday, D. D. C. Bradley, P. L. Burn, R. H. Friend, and A. B. Holmes, J. Phys.: Condens. Matter **5**, 7155 (1993).
[58] R. Osterbacka, M. Wohlgenannt, M. Shkunov, D. Chinn, and Z. V. Vardeny, J. Chem. Phys. **118**, 8905 (2003).
[59] L. J. Rothberg, M. Yan, F. Papadimitrakopoulos, M. E. Galvin, E. W. Kwock, and T. M. Miller, Synth. Met. **80**, 41 (1996).
[60] N. T. Harrison, G. R. Hayes, R. T. Phillips, and R. H. Friend, Phys. Rev. Lett. **77**, 1881 (1996).
[61] D. Comoretto, F. Marabelli, P. Tognini, A. Stella, and G. Dellepiane, Synth. Met. **119**, 643 (2001).
[62] D. Comoretto, G. Dellepiane, G. F. Musso, R. Tubino, R. Dorsinville, A. Walser, and R. R. Alfano, Phys. Rev. B **46**, 10041 (1992).
[63] D. Comoretto, G. Dellepiane, C. Cuniberti, L. Rossi, A. Borghesi, and J. LeMoigne, Phys. Rev. B **53**, 15653 (1996).
[64] J. Wery, H. Aarab, S. Lefrant, E. Faulques, E. Mulazzi, and R. Perego, Phys. Rev. B **67**, 115202 (2003).
[65] R. Osterbacka, M. Wohlgenannt, D. Chinn, and Z. V. Vardeny, Phys. Rev. B **60**, R11253 (1999).
[66] E. Mulazzi, A. Ripamonti, J. Wery, B. Dulieu, and S. Lefrant, Phys. Rev. B **60**, 16519 (1999).
[67] N. T. Harrison, D. R. Baigent, I. D. W. Samuel, R. H. Friend, A.

C. Grimsdale, S. C. Moratti, and A. B. Holmes, Phys. Rev. B **53**, 15815 (1996).
[68] G. R. Hayes, I. D. W. Samuel, and R. T. Phillips, Phys. Rev. B **52**, 11569 (1995).
[69] R. Kersting, U. Lemmer, R. F. Mahrt, K. Leo, H. Kurz, H. Bassler, and E. O. Gobel, Phys. Rev. Lett. **70**, 3820 (1993).
[70] L. S. Swanson, J. Shinar, A. R. Brown, D. D. C. Bradley, R. H. Friend, P. L. Burn, A. Kraft, and A. B. Holmes, Phys. Rev. B **46**, 15072 (1992).
[71] D. A. Halliday, P. L. Burn, R. H. Friend, D. D. C. Bradley, A. B. Holmes, and A. Kraft, Synth. Met. **55**, 954 (1993).
[72] T. Q. Nguyen, V. Doan, and B. J. Schwartz, J. Chem. Phys. **110**, 4068 (1999).
[73] G. H. Meeten, *Optical Properties of Polymers* (Elsevier Applied Science Publishers, London, 1986).
[74] O. Inganas, in *Organic Photovoltaic*, edited by C. J. Brabec, V. Dyakonov, J. Parisi, and S. N. Sariciftci (Springer, Berlin, 2003).
[75] M. Galli, F. Marabelli, and D. Comoretto, Appl. Phys. Lett. **86**, 201119 (2005).
[76] G. F. Bassani and G. Pastori Parravicini, *Electronic States and Optical Transitions in Solids* (Pergamon Press, New York, 1975).
[77] J. R. Lakowicz, *Principles of Fluorescence Spectroscopy* (Kluwer Academic/Plenum, New York, 1999).
[78] A. Röseler, *Infrared Spectroscopic Ellipsometry* (Akademie-Verlag, Berlin, 1990).
[79] G. Masetti, E. Campani, G. Gorini, R. Tubino, P. Piaggio, and G. Dellepiane, Chem. Phys. **108**, 141 (1986).
[80] G. L. J. A. Rikken, Physica B **204**, 353 (1995).
[81] J. B. Birks, *Photophysics of Aromatic Molecules* (Wiley-Interscience, London, 1970).
[82] A. Gigli Berzolari, *Introduzione all'Elettromagnetismo* (La Goliardica Pavese, Pavia, 1970).
[83] G. L. J. A. Rikken and Y. A. R. R. Kessener, Phys. Rev. Lett. **74**, 880 (1995).
[84] M. Tammer, R. W. T. Higgins, and A. P. Monkman, J. Appl. Phys. **91**, 4010 (2002).
[85] G. R. Fowles, *Introduction to Modern Optics* (Dover, New York, 1989).
[86] C. H. Lee, J. Y. Park, Y. W. Park, D. Moses, A. J. Heeger, T. Noguchi, and T. Ohnishi, Synth. Met. **101**, 444 (1999).
[87] D. D. C. Bradley and R. H. Friend, J. Phys.: Condens. Matter **1**, 3671 (1989).
[88] Y. V. Romanovskii, V. I. Arkhipov, and H. Bassler, Phys. Rev. B **64**, 033104 (2001).
[89] S. H. Lim, T. G. Bjorklund, and C. J. Bardeen, J. Chem. Phys. **118**, 4297 (2003).
[90] D. Moses, H. Okumoto, C. H. Lee, A. J. Heeger, T. Ohnishi, and T. Noguchi, Phys. Rev. B **54**, 4748 (1996).
[91] D. Moses, A. Dogariu, and A. J. Heeger, Phys. Rev. B **61**, 9373 (2000).
[92] P. B. Miranda, D. Moses, and A. J. Heeger, Phys. Rev. B **64**, 081201 (2001).
[93] G. Lanzani (private communication).
[94] M. Furukawa, K. I. Mizuno, A. Matsui, S. Rughooputh, and W. C. Walker, J. Phys. Soc. Jpn. **58**, 2976 (1989).
[95] C. Soci, D. Moses, Q. H. Xu, and A. J. Heeger, Phys. Rev. B **72**, 245204 (2005).
[96] E. Mulazzi, R. Perego, J. Wery, L. Mihut, S. Lefrant, and E. Faulques, J. Chem. Phys. **125**, 014703 (2006).
[97] H. Baessler, in *Primary Photoexcitations in Conjugated Polymers: Molecular Excitation versus Semiconductor Band Model*, edited by N. S. Sariciftci (World Scientific, Singapore, 1997).
[98] M. Muccini, E. Lunedei, A. Bree, G. Horowitz, F. Garnier, and C. Taliani, J. Chem. Phys. **108**, 7327 (1998).
[99] C. Y. Yang, K. Lee, and A. J. Heeger, J. Mol. Struct. **521**, 315 (2000).
[100] J. Cornil, D. A. dos Santos, X. Crispin, R. Silbey, and J. L. Bredas, J. Am. Chem. Soc. **120**, 1289 (1998).
[101] A. Ferretti, A. Ruini, E. Molinari, and M. J. Caldas, Phys. Rev. Lett. **90**, 086401 (2003).
[102] K. Hummer and C. Ambrosch-Draxl, Phys. Rev. B **72**, 205205 (2005).
[103] I. B. Martini, A. D. Smith, and B. J. Schwartz, Phys. Rev. B **69**, 035204 (2004).
[104] T. Offermans, P. A. van Hal, S. C. J. Meskers, M. M. Koetse, and R. A. J. Janssen, Phys. Rev. B **72**, 045213 (2005).
[105] R. D. Schaller, L. F. Lee, J. C. Johnson, L. H. Haber, R. J. Saykally, J. Vieceli, I. Benjamin, T. Q. Nguyen, and B. J. Schwartz, J. Phys. Chem. B **106**, 9496 (2002).
[106] D. T. McQuade, J. Kim, and T. M. Swager, J. Am. Chem. Soc. **122**, 5885 (2000).